Post-processing algorithm for damped and step-change events detection in PMUs signal

Sanjay Singh Negi
Indian Railways,
Allahabad, India
Email:kinnaursanjay@yahoo.co.in

Nand Kishor
Dept. of Elect. Engg.
MNNIT Allahabad, India
Email:nand_research@yahoo.co.in

Kjetil Uhlen
NTNU, Trondheim
Norway
Email: kjetil.uhlen@ntnu.no

Richa Negi
Dept of Elect. Engg.
MNNIT Allahabad, India
Email: richa@mnnit.ac.in

***Abstract*— The study presents an algorithm using signal processing techniques to screen PMUs data for events. The algorithm can be applied on multiple PMUs data for possible events detection and their display. The algorithm analyze the each moving window frame, i.e. segment of selected samples. The signal processing technique is based on decomposition of each segment via empirical mode decomposition followed by calculation of statistical indices on sum of intrinsic mode functions (IMFs)/square-root of spectral kurtosis computed on IMFs. The maximum energy content computed for each segment of PMUs signal signifies the presence of any event of damped transient, step-change/impulse or even normal condition.**

***Index Terms*—Event detection, PMUs, Spectral kurtosis**

I. Introduction

Wide area monitoring is an emerging technology that can aggregate the interconnected power grid with measurements of signals via PMUs at centralized location. While a number of phasor technology applications have already been developed and as users gain experience, new applications will continue to be explored with additional tools being developed. There is a need to implement visualization techniques, advanced algorithms and intelligent tools to provide useful insights in avoiding major system disturbances. The grid operators expect using such tools to quickly present the received PMU data in the form of actionable intelligence [1]. In past one decade, significant research contributions on event detection have been focused. These events can be due to any kind of disturbance like, generation loss, transmission line loss, change in active/reactive power flow and any other operating conditions in the power system. The events following such disturbances provide greater information on the dynamics, system inertia, power supply-demand mismatch, etc. Analysis of events will provide understanding of system behavior under wide range of operating conditions.

Several researchers have reported their study related to event detection using PMUs data. The use of finite impulse response (FIR) filtering [2] for transient event, algorithms based on Fourier transforms and Yule Walker methods [3-4] towards screening of large volume of data for events are described. The study [5] presented generator clustering approach to determine the source of an event based on detecting the largest initial rotor swing.

The dimensionality reduction for a large set of PMUs data and event detection using principal component analysis (PCA) is reported in [6]. The approach is based on performance index defined in terms of prediction error calculated under normal operating conditions of the power system. An event alert gets issued whenever performance index becomes larger than pre-specified threshold. A two-stage framework supported with monitoring and real-time analysis and PMU data management is addressed in study [7]. The events in the data are identified from streams of PMUs using correlation index matrix, while bitmap is applied to compress.

Application of advanced signal processing is an ideal tool for the task of automating the analysis of measured PMUs data. In [8], authors discuss event detection scheme using statistical measures, residual modeling, STFT and slope for phase angle difference signal. In their study, however, justification on choice of threshold to reach make event decision is supported.

This paper focuses on event detection based on the continuous data stream collected via PMUs installed at different locations in the power grid. The proposed event detection consists of two steps: 1) to detect an event within each data segment (or window) and 2) to locate the time-instant of change for the event.

This paper is organized as follows. The signal processing techniques adopted in algorithm is described in Section II, followed by proposed event detection algorithm in Section III. The description of case studies on PMUs data used in study are detailed in Section IV. In the next Section V, the results are discussed on the performance of proposed scheme and finally, the conclusions drawn in Section VI.

Identify applicable sponsor/s here. *(sponsors)*

II. POST-PROCESSING TECHNIQUES

This section presents the signal processing techniques that are applied for detection of events and quantify the dynamics of signals following the disturbances.

A. Empirical mode decomposition (EMD):

The EMD first introduced by Huang et al. [9] is capable to adaptively decompose any signal into a set of L_I level of complex-valued oscillating components, known as intrinsic mode functions (IMFs) and a residual representing the trend. These IMFs define the phase information for the real and imaginary components locally. Mathematically, the set of IMFs $\{I_l(t)\}_{l=1}^{L_I}$ and a residual value is expressed as:

$$S(t) = \sum_{l=1}^{L_I} I_l(t) + r(t) \tag{2}$$

The IMFs extraction from the segment is based on an iterative method known as shifting algorithm and it can found in [10].

B. Spectral Kurtosis:

In simple terms, spectral kurtosis (SK) is defined as the normalised fourth-order moment of the real part of the short-time Fourier transform [11]. The SK is an extension of statistical measure of kurtosis defining the impulsivity of the event in the signal in the frequency domain. The SK is computationally less expensive and fast, and thus suitable for on-line applications. Wold-Cramer's decomposition describes any stationary stochastic process as the output of a causal, linear, and time-invariant system excited by strict white noise.

$$S(t) = \int_{-\infty}^{t} h(t-\tau)U(\tau)d\tau \tag{3}$$

For non-stationary signal, $h(t,s)$ refers to causal impulse response at time t of a system excited by an impulse at time $t-s$, then

$$S(t) = \int_{-\infty}^{t} h(t,t-\tau)U(\tau)d\tau \tag{4}$$

In frequency domain, above equations becomes

$$S(t) = \int_{-\infty}^{\infty} e^{j2\pi ft} H(t,f)dU(f) \tag{5}$$

Where, $H(t,f)$ is time-varying transfer function of the system, which may be assumed as the complex envelope signal $S(t)$ at frequency point f. Consider $H(t,f)$ conditioned at given ω, a random variable of filter's time-varying characteristic. Subsequently, the second-order instantaneous moment that measures the strength of the energy of the complex envelope at time t and frequency f can be given as:

$$M_{2nS}(t,f) = \frac{E\{|H(t,f)dU(f)|^{2n}\omega\}}{df} = |H(t,f)|^{2n} M_{2nU} \tag{6}$$

The defined instantaneous moment decomposes the energy contained in $S(t)$ over the TF plane (t,f) at $n=1$.

Now, the fourth-order spectral cumulant of a non-stationary signal can be given as

$$C_{4S}(f) = M_{4S}(f) - 2M_{2S}^2(f)\ , f \neq 0 \tag{7}$$

A larger deviation of signal from Gaussianity results into larger value of above equation. Ideally, SK assumes zero values at those frequencies corresponding to stationary Gaussian noise and high positive values at frequencies accompanied by transients like events in the signals [12].

The SK is defined as

$$K_S(f) = \frac{C_{4S}(f)}{M_{2S}(f)} = \frac{C_{4S}(f)}{M_{2S}^2(f)} - 2\ , f \neq 0 \tag{8}$$

The square-root of SK (SRSK) is computed on the sum of IMFs after decomposition of segment via applying EMD technique.

III. EVENT DETECTION SCHEME

An early awareness on the grid situation reaching a vulnerable state is an indication of event. This calls analytical tools to recognize the condition and implement corrective actions, in order to mitigate potential risks for reliable grid operations. The raise of alarm on the occurrence of a particular event, will trigger the online estimation of state dynamics [13].

A. Segment Processing

As the volume of PMUs data increases, it is equally important not only to compress the data for optimizing the storage requirement [14] but also to concisely visualize on the operator's screen. Consider a large scale PMUs N_p deployment in wide-spread power grid network, each providing q measured signals. In real-time monitoring and analysis stage, the PMU data from phasor data concentrator is received. Typically, a PMU provides (measured and calculated) $q = 5$ time series bus signals; frequency (F), active power (P), reactive power (Q), voltage angle (A) and voltage magnitude (V). A total of $z = N_p \times q(t')$ measurements is thus collected at every time instant. The architecture for event detection in PMUs signals is depicted in Fig. 1. As illustrated, the PMUs time series data is considered to have a segment of finite size of samples m. The PMUs data is segmented into fixed-length window of m samples being available at a rate of 50 or 60 Hz defining a total time length of T sec. Each segment $S = [\vartheta_1\ \vartheta_2 \dots \vartheta_m]$ is a sequence of samples ϑ_i from time series PMU data. Once the length of initial data segment equals to selected size of samples, the detection algorithm is initiated. The event detection algorithm is applied on each segmented data for possible events. The algorithm determines if the new data segment in analysis has characteristics which represent an event. We must be able to discriminate between normal and events conditions. For each event detected from the different signals (F, P, Q, A or V) during the operating time of algorithm, it should be possible discriminate event against normal conditions.

In the selected window segment, using EMD technique, decomposed IMFs I_l of levels L_I are evaluated. Here L_I refers to total level of IMFs minus residue level obtained while decomposition using EMD. The sum of L_I level of IMFs is performed. At this stage, algorithm gets bifurcated into two stages. In the first stage, square-root of SK (SRSK) is obtained for the sum of L_I level of IMFs. Next, absolute envelope using Hilbert transform of SRSK is determined followed by calculation of statistical indices. While in second stage, absolute envelope is determined directly from sum of L_I level of IMFs followed by calculation of statistical indices.

Thus, in order to identify the presence of step-change/impulse in the PMUs signal, the combination of EMD and SK is applied to calculate the statistical indices following the determination of absolute envelope of SRSK. On the other hand, confirmation on damped transient type event in the PMUs signal is obtained from calculation of indices directly from absolute envelope of sum of IMFs. The computed statistical signatures on the analysis segment are compared with those obtained on previous segment.

B. Computation of Event Indices

In order to detect event in the segment, indices; maximum of energy content is calculated from the absolute envelope of SRSK and sum of IMFs. The transient/step-change event types in the PMUs signal calls for alerts or shut down and proves suitable in real-time implementation. Considering decomposition of segment into L_I level IMFs, their sum is performed using

$$SUM_I(z;m;L_I) = \sum_{l=1}^{L_I} I_l$$

As described above, after this stage, algorithm is bifurcated into two stages. In the first stage, SRSK is computed from the sum of IMFs given as

$$K_{SRSK}(m) = \sqrt{K_s(m)}$$

The temporal envelope $ENV(m)$ of the signal is derived from the amplitude of analytic signal of SRSK, $K_{a,SRSK}(m)$ or sum of IMFs $SUM_{a,I}(m)$ given by its Hilbert transform. In other words, its absolute envelope for one of the PMU signal, $q = 1$ is determined by applying Hilbert transform, followed by magnitude in MATLAB and given as:

$$ENV_{SRSK}(m) = abs(hilbert(K_{a,SRSK}(m)))$$

The energy content is now computed using

$$E_{SRSK}(m) = |ENV_{SRSK}(m)|^2 \tag{12}$$

Similarly, RMSE and maximum energy content is given as

$$RMSE_{SRSK} = \sqrt{\frac{1}{m} E_{SRSK}(m)},$$

$$E_{SRSK}^{max} = Max\{E_{SRSK}(m)\} \tag{13}$$

While in second stage, as discussed above, envelope is directly computed from sum of IMFs, i.e.

$$ENV_I(m) = abs(hilbert(SUM_{a,I}(m)))$$

And energy content is computed from

$$E_I(z;m) = |ENV_I(m)|^2 \tag{12}$$

Similarly, RMSE and maximum energy content is given as

$$RMSE_{IMF} = \sqrt{\frac{1}{m} E_I(z;m)} \;\&\; E_{IMF}^{max} = Max\{E_I(z;m)\} \tag{13}$$

IV. PMUs Data Case Studies

The voltage angle PMUs signals are used to screen the presence of any event. However, other signals too can be utilized to detect power system events.

A. NASPI PMU Data

The accessed NASPI PMUs data (at 60 Hz) is analyzed according to the grid interconnections between the regions. The angle difference signal between the regions; R-1 (Central-South angle: CSA), R-2 (North-South angle: NSA), R-3 (West-South angle: WSA) & R-4 (West-East angle WEA) clearly suggests the impulse event, masked by oscillations as shown in Fig. 2. Each region reflect five distinct events; A, B, C, D & E with regard to its characteristic. These events of one region are synchronized with the event characteristic of other regions. It may be seen these events are associated with significantly higher magnitude against non-event, i.e. post-event period. The analysis is performed on each data segment consisting of 1000 samples corresponding to event and post-event duration.

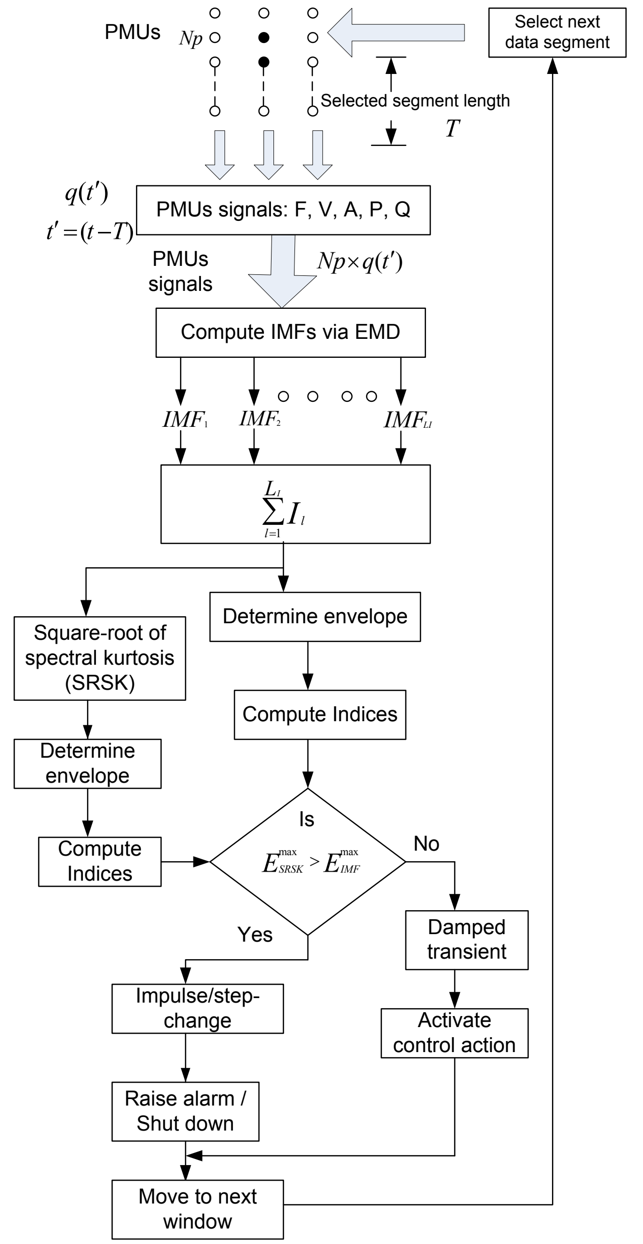

Figure 1. Flow chart illustrating the implementation of event detection

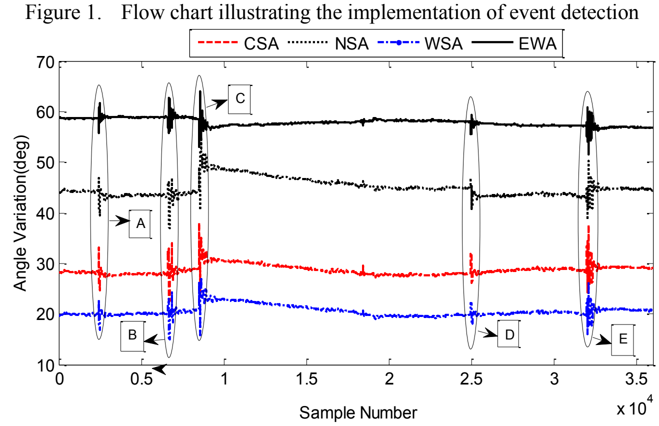

Figure 2. Voltage angle variation of NASPI PMUs data

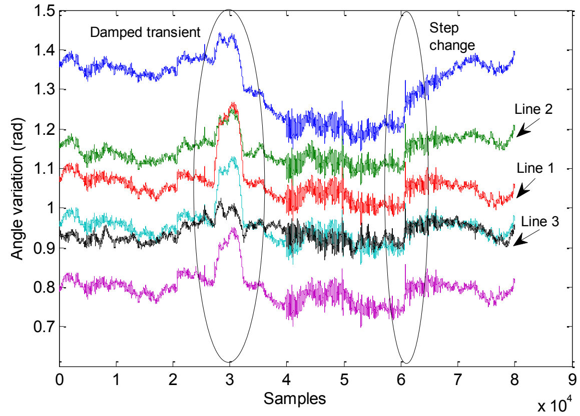

(a) Angle variation

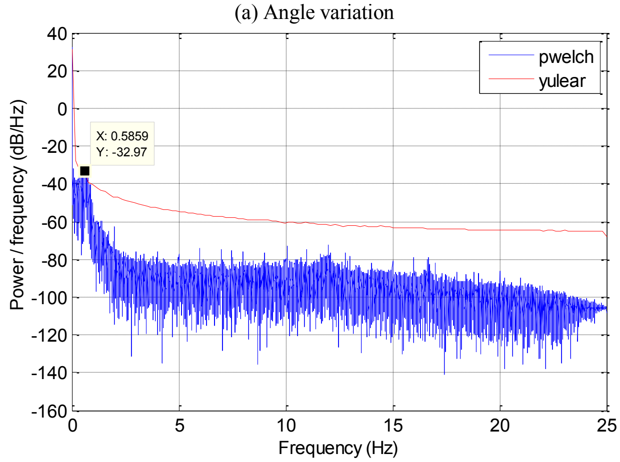

(b) Spectral analysis for Line 1 signal

Figure 3. Angle signal of Nordic grid and its property

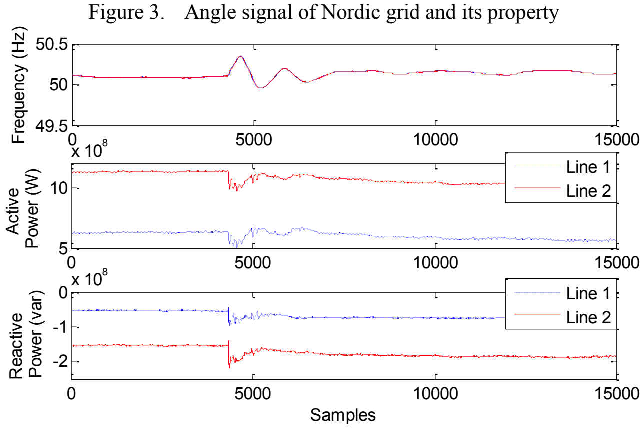

Figure 4. PMUs signals variation for case II

B. *Nordic grid PMUs data*

Another time-series collected data considered in study is from Nordic grid for test case I & II. The PMUs signal is sampled at 50 Hz. The collected signals of case I, accompanied with some events are shown in Fig. 3. The synchrophasor data have variety of events such as step change and damped transient type. The event of step change type is associated with step change in angle signal from one value to high/low value. The voltage phase angle of each PMU is unwrapped before the difference of the voltage angle between the two PMUs is taken. It is also clear, between the two events as indicated in said figure, the angle signal has stronger higher magnitude oscillations. The spectral analysis of angle difference, i.e. Line 1 suggests a strong mode of 0.5859 Hz.

The variation of signals for case II is shown in Fig. 4. It is indicated that loading of line 2 is more than line 1. The events associated with real power disturbance primarily leads to transient in frequency and voltage magnitude signals while, reactive power affects the voltage magnitude (locally) only [15].

V. Results And Discussion

A. *Analysis on NASPI data*

The above discussed event detection algorithm is applied on window segment of 1000 samples and computed SRSK corresponding to event/post-event condition is illustrated in Fig. 5. As indicated in Fig. 5(a), such event is of impulse category of very short duration. The SRSK specifies the impulse accurately having high magnitude during the event period. During the post-event period, the signal returns to normal conditon and SRSK magnitude is also in the same range as original one. The calculated absolute envelope from SRSK and IMFs is shown in Fig. 6. It is clear for this type of event, maximum energy calculated from envelope of SRSK is of higher magnitude than those obtained from sum of IMFs.

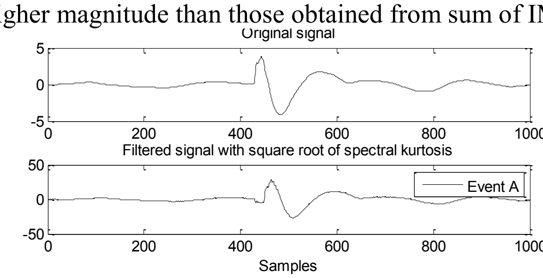

(a) SRSK for event-A

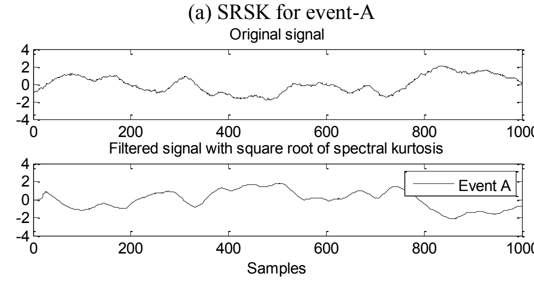

(b) SRSK for post-event-A

Figure 5. Computed SRSK for event-/post-event-A of region R1

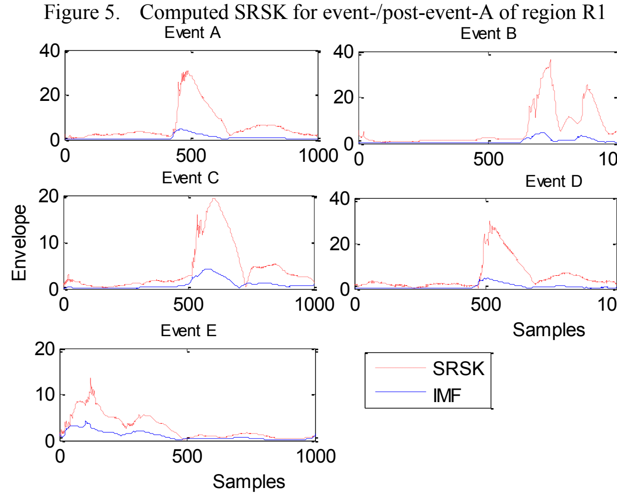

(a) Event conditions

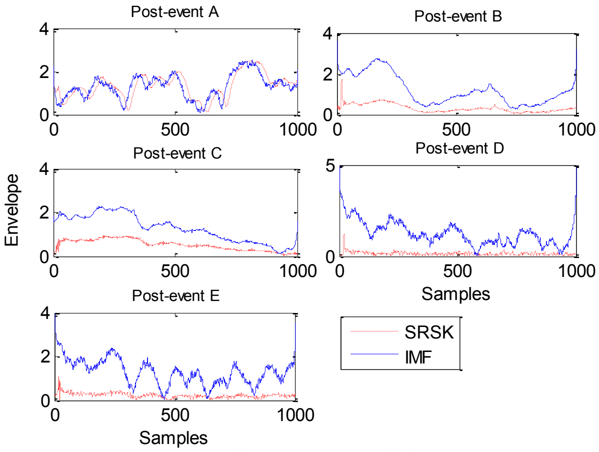

(b) Post-event conditions

Figure 6. Calculation of absolute envelope of voltage angle signals of region R3

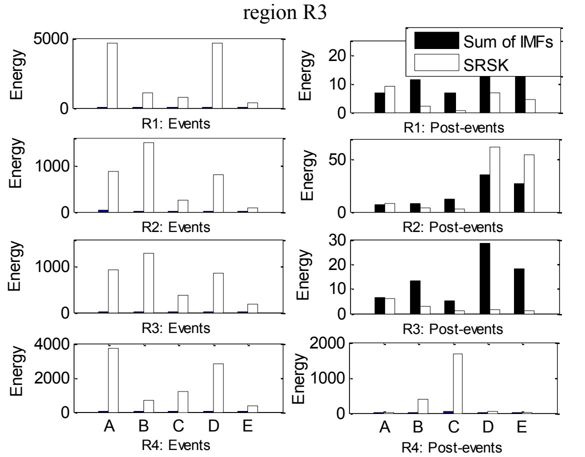

Figure 7. Maximum energy for events/post-events of different regions

It is expected that if an event is present in the particular segment, the maximum energy content would be significantly higher than those calculated for non-event segment. In contrast, for post-event condition in R3, those determined from sum of IMFs is higher than SRSK. On other hand, for region R1, the higher magnitude of sum of IMFs with respect to SRSK suggested in Fig. 7 signifies that damped transient event has die-out followed by oscillations during post-event conditions; B, C, D and E.

B. Analysis on Nordic grid data

For case I, as observed in Fig. 8(a), the envelope computed on SRSK and sum of IMFs alone, suggests that lines 1 and 2 are associated with step change event at 7th segment respectively. On other hand, similar events are observable not only in 7th segment but also in 4th segment on line 3. In study, possible events are detected and analyzed by calculating instantaneous energy for all the window segment of complete length of PMU data. The step-change event signatures (instantaneous energy) obtained by SRSK is noticeable at 7th segment in Fig. 8(b). This also becomes clear from maximum energy content for 7th segment as shown in shown in Fig. 8(c). It is worth noting that the in the 4th segment, maximum energy content calculated from IMF becomes close to those of SRSK on line 3. An event is suspected in 4th segment. This is due to fact that there is damped transient type event in angle signal. In other words, the envelope of 4th segment indicates a step change, however, indices calculated confirms damped transient type event since, its value is larger than those of SRSK. In the analysis of Nordic grid data, referring to Case II, as illustrated in Fig. 9, step change variation is suggested in reactive power signal on line 1 and extends to next segment on line 2. On other hand, energy computed from sum of IMF is larger than SRSK in the 6th segment of active power signal. The damped transient event is suggested here.

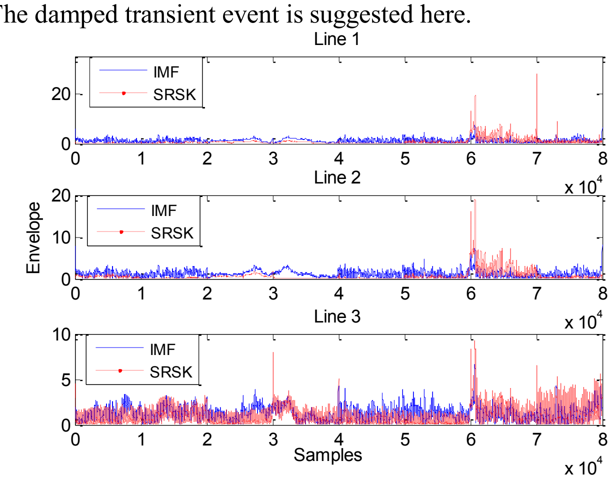

(a) Absolute envelope

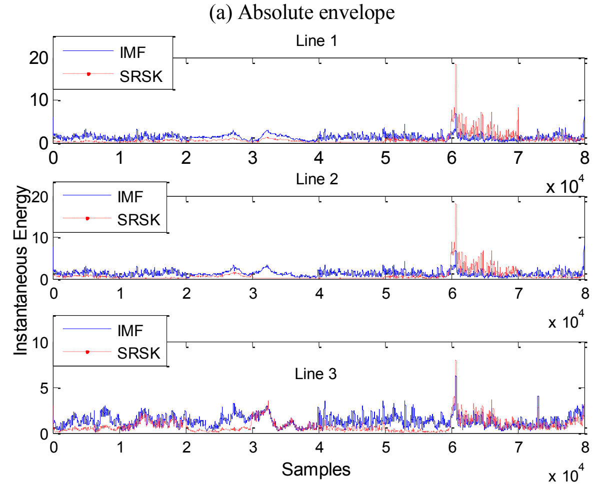

(i) Detailed plot

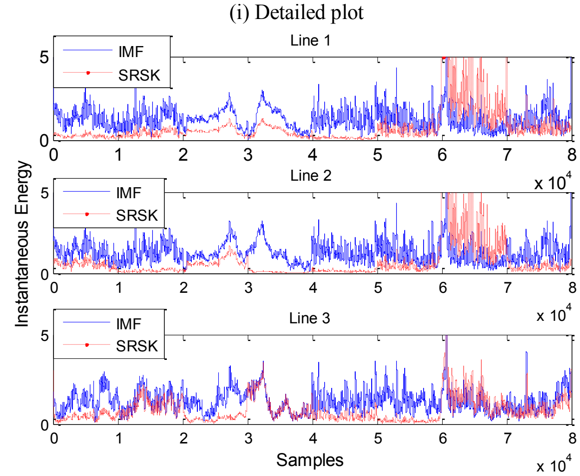

(ii) Zoomed plot

(b) Instantaneous energy

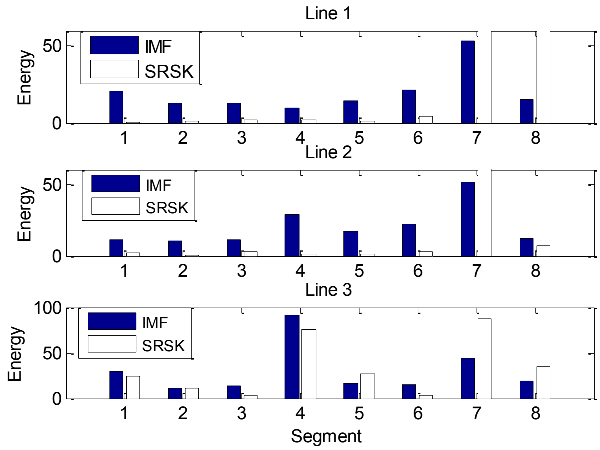

(c) Maximum energy content

Figure 8. Calculated indices for event detection of Case I

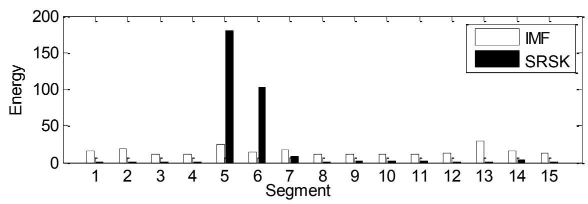

(a) Reactive power signal- Line 1

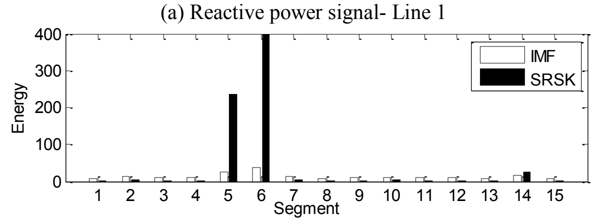

(b) Reactive power signal - Line 2

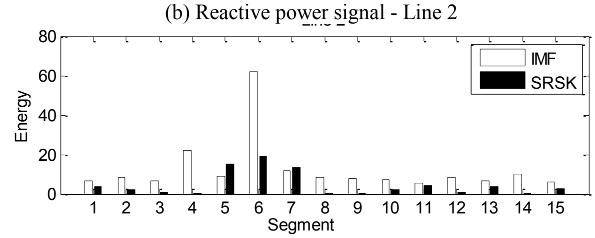

(c) Active power signal - Line 2

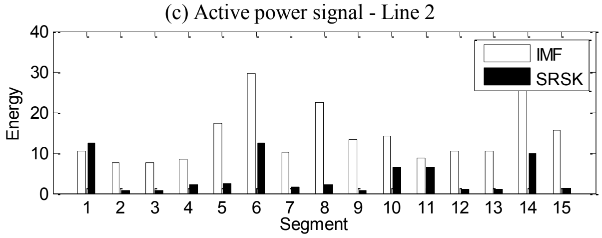

Frequency signal

Figure 9. Calculated indices for event detection of Case II

The maximum energy of sum of IMFs/SRSK is eventually zero when a suspected event is not found, i.e. when normal state exists in the system. It is important to investigate how the event is propogated to lines from the point of event occurrence in the system, which is not discussed in this paper. Further, energy computed using sum of IMFs of frequency signal too is higher than SRSK. Specifically, significant magnitude of energy is found for every segment of frequency signal, indicating its sensitivity to system disturbance.

VI. Conclusion

The paper discussed calculation of indices from sum of IMF and SRSK to analyze damped transient and step change type of events. Several PMUs signals were considered to undertand the event characteristics. In future scope, some other PMUs signals needs to be investigated to understand the event characterictics and their sensitivity.

Acknowledgment

The authors acknowledge the receipt of research support on project "Operation of the Smart Grid with Wide Area Information (OperaGrid)" by DST-RCN of the two countries (Indo-Norway Joint Proposal).

References

[1] D. Novosel, V. Madani, B. Bhargava, K. Vu, J. Cole, Dawn of the grid synchronization, *IEEE Power and Energy Magazine*, Vol.6, no. 1,pp. 49-60, 2008.

[2] J. E. Tate, "Event detection and visualization based on phasor measurement units for improved situational awareness," Ph.D. dissertation, Dept.Elect. Comput. Eng., Univ. Illinois, Urbana-Champaign, IL, USA, 2008.

[3] S. Sohn, A. J. Allen, S. Kulkarni, W. M. Grady, and S. Santoso, "Event detection method for PMUs synchrophasor data," in *Proc. IEEEConf. Power Electron. Mach. Wind Appl. (PEMWA)*, Denver, CO, USA, Jul. 2012, pp. 1–7.

[4] A. J. Allen, S. Sohn, S. Santoso, and W. M. Grady, "Algorithm for screening PMU data for power system events," in *Proc. IEEE Int. Conf.Innov. Smart Grid Technol.*, Berlin, Germany, Oct. 2012, pp. 1–6.

[5] K. Mei, S. M. Rovnyak, and C. Ong, "Design aspect for wide-area monitoring and control system," *IEEE Trans. Power Syst.*, vol. 23, no. 2, pp. 673–679, May 2008.

[6] Yang Chen, Le Xie, P. R. Kumar, Dimensionality reduction and early event detection using online synchrophasor data, *IEEE Trans. on Power System*, Vol. 29, No. 6, pp. 2784-2794, 2014.

[7] Ben McCamish et al., A data driven framework for real-time power system event detection and visualization, arXiv:1501.04038

[8] S-W Sohn, A.J. Allen, S. Kulkarni, W. M. Grady, and S. Santoso, Event Detection Method for the PMUs Synchrophasor Data, in *Proc. of IEEE Power Electronics and Machines in Wind Applications*, pp. 1-7, 16-18 July 2012, Denver, CO, 2012.

[9] N. E. Huang, et al. The empirical mode decomposition and the Hilbert spectrum for nonlinear and non-tationary time series analysis. Proceedings of the Royal Society of London, Series A, 454, pp. 903-995, 1998.

[10] P. Flandrin, G. Rilling, and P. Goncalves, Empirical mode decomposition as a filter bank, IEEE Signal Processing Letters, Vol. 11, no. 2, pp.112–114, 2004.

[11] J. Antoni, The spectral kurtosis: a useful tool for characterising non-stationary signals, Mechanical Systems and Signal Processing, Vol. 20, pp. 282–307, 2006.

[12] J. Antoni, R.B. Randall, The spectral kurtosis: application to the vibratory surveillance and diagnostics of rotating machines, Mechanical Systems and Signal Processing, Vol. 20, pp. 308–331, 2006.

[13] P. M. Ashton *et al.*, Novel application of detrended fluctuation analysis for state estimation using synchrophasor measurements, *IEEE Trans.Power Syst.*, vol. 28, no. 2, pp. 1930–1938, 2013.

[14] J. Cormane, F. A. O. Nascimento, *Spectral shape estimation in data compression for smart grid monitoring, IEEE Trans. on Smart Grid*, Vol 7, No. 3, pp. 1214-1221, 2015.

[15] D-I. Kim, T. Y. Chun, S. H. Yoon, G. Lee, and Y.-J. Shin, Wavelet-Based Event Detection Method Using PMU Data, *IEEE Transactions on Smart grid*, online published, 2015.